

## N O T I C E

THIS DOCUMENT HAS BEEN REPRODUCED FROM  
MICROFICHE. ALTHOUGH IT IS RECOGNIZED THAT  
CERTAIN PORTIONS ARE ILLEGIBLE, IT IS BEING RELEASED  
IN THE INTEREST OF MAKING AVAILABLE AS MUCH  
INFORMATION AS POSSIBLE

JAN 42 1975

Hold Reading  
Rabl.

12/1-17-75

EXPERIMENTAL FEASIBILITY STUDY OF THE APPLICATION OF  
MAGNETIC SUSPENSION TECHNIQUES TO LARGE-SCALE AERODYNAMIC TEST FACILITIES\*

Ricardo ~~N. Zapata~~  
Associate Professor, Department of Engineering Science and Systems

Robert R. Humphris  
Senior Scientist and Lecturer, Department of Engineering Science and Systems

Karl C. Henderson  
Research Engineer, Department of Electrical Engineering

University of Virginia  
Charlottesville, Virginia 22901



Abstract

Based on the premises that (1) magnetic suspension techniques can play a useful role in large scale aerodynamic testing and (2) superconductor technology offers the only practical hope for building large scale magnetic suspensions, an all-superconductor 3-component magnetic suspension and balance facility was built as a prototype and tested successfully at the University of Virginia. Quantitative extrapolations of design and performance characteristics of this prototype system to larger systems compatible with existing and planned high Reynolds number facilities at Langley Research Center have been made and show that this experimental technique should be particularly attractive when used in conjunction with large cryogenic wind tunnels.

Introduction

Electromagnetic suspension techniques have been applied to support models in aerodynamic facilities for nearly 20 years (1),(2),(3). The two main advantages of these techniques, i.e., interference-free model support and the ability to infer aerodynamic forces from measurements of electric current in the supporting coils, have been exploited successfully by several experimenters in this country and in Europe for a variety of interesting applications including studies in low-density aerodynamics, hypersonic wakes, dynamic stability of 2- and 3-dimensional shapes, etc. (4).

Considering the intrinsic advantages of magnetic suspensions, it might appear to be somewhat puzzling that this technique has not been adopted more universally than it has. Undoubtedly, the technological complexity of the technique, for example requiring the presence of automatic controls talent in the experimental team, has been somewhat of a deterrent. But, that could hardly be a satisfactory explanation in recent years given the level of sophistication of other types of instrumentation used in aerodynamic test laboratories and the high technical level of the personnel working there. The real difficulty appears to have been associated with the scalability of practical magnetic suspension devices to fit the large-scale test facilities needed for realistic Reynolds number simulation. And, considering the increasing emphasis on Reynolds number as a critical aerodynamic simulation parameter in recent years, it can be safely predicted that the

future of electromagnetic suspension as an aerodynamic testing technique will be decided largely on the basis of the feasibility of using such experimental technique in conjunction with high Reynolds number testing.

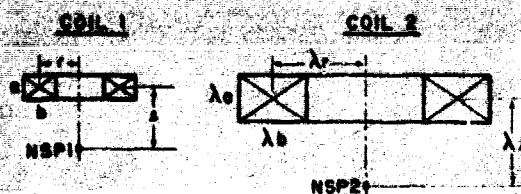
In 1966, Parker (5) derived simple scaling laws for conventional magnetic suspension coils. His findings are summarized in Figure 1, where a simple spherical model is used as a reference and where scaling laws are given for both model magnetization coils and gradient, or force-producing coils. From these simple scaling laws, Parker concluded that the most promising approach to applying magnetic suspension techniques to large facilities consisted of using magnets built of low resistivity conductors. This realization led to the "cold balance" concept, initially conceived around high purity conductors operated at extremely low temperatures (supercooled) and subsequently evolving towards the utilization of superconductors. A critical question remained to be resolved, i.e., whether or not superconductors could be used economically in the highly dynamic mode of operation characteristic of wind tunnel magnetic suspensions.

For the past seven years a prototype cold magnetic suspension and balance facility, utilizing state-of-the-art superconductor technology has been under development at the University of Virginia. At the start of this project two main objectives were formulated: (1) to study the feasibility of applying a quasi 6-degree-of-freedom free support technique to dynamic stability research; (2) to investigate design concepts and parameters that are critical for applying magnetic suspension techniques to large-scale aerodynamic facilities. A symmetric 3-component magnetic balance configuration was chosen to promote the first stated objective. In line with the second objective, an all-superconductor coil assembly became the logical choice, after a thorough study of available technologies revealed that superconductors offer the only realistic hope for building large-size magnetic suspension systems.

This paper reports on important results relevant to the second stated project objective. In the following sections brief descriptions of design and operational characteristics of the prototype facility are given. Next, scaling characteristics of superconductor coil systems are discussed and a preliminary design extrapolation to a medium-scale facility compatible with NASA Langley's high Reynolds number cryogenic transonic tunnel is sketched. Further

\*Work supported under NASA grants NGR 47-005-029, NGR 47-005-110, NGR 47-005-112 and NSG 1010.

extrapolation to a large-scale facility compatible with Langley's transonic research tunnel is explored. Conclusions and recommendations are offered at the end of the paper.



COIL	1	2
CONDUCTOR RESISTIVITY	$\rho_1$	$\rho_2$
CURRENT DENSITY	$J_1$	$J_2$

AT NOMINAL SUSPENSION POINT (NSP):

$$\text{MAGNETIC FIELD } \frac{B_2}{B_1} = \left( \frac{J_2}{J_1} \right) \lambda$$

$$\text{MAGNETIC FIELD GRADIENT } \frac{\nabla B_2}{\nabla B_1} = \frac{J_2}{J_1}$$

$$\text{COIL VOLUME, WEIGHT} \propto \frac{V_2}{V_1} = \frac{W_2}{W_1} = \lambda^3$$

$$\text{JOULIAN POWER DISSIPATION } \frac{P_2}{P_1} = \left( \frac{J_2}{J_1} \right)^2 \left( \frac{\rho_2}{\rho_1} \right) \lambda^3$$

$$\text{AMPERE} \times \text{TURNS } \frac{NI_2}{NI_1} = \left( \frac{J_2}{J_1} \right) \lambda^2$$

\* assumes equal coil densities.

Fig. 1 Coil Scaling Laws

### Facility Description

The prototype facility consists of a combination of a supersonic wind tunnel and a superconductor magnetic suspension and balance. Design and implementation details of elements of these major facility components may be found in paper A of reference 3. Here only brief descriptions directly relevant to operating characteristics are given.

### The Wind Tunnel

A blow-down wind tunnel with a contoured Mach 3 nozzle, 5.75 in. test section diameter, atmospheric exhaust is used. 2000 cu. ft. of air can be stored at 275 psi, atmospheric temperature, typically giving one 4-minute run at 50 psia stagnation pressure every 90 minutes. To increase run time and decrease aerodynamic loads on the suspended models an optimized variable second throat arrangement is employed, which permits tunnel operation at 41 psia stagnation pressure with a 1 in. spherical model. Figure 2 is a sketch of the facility which illustrates the relative size and location of wind tunnel components vis-a-vis magnetic suspension components.

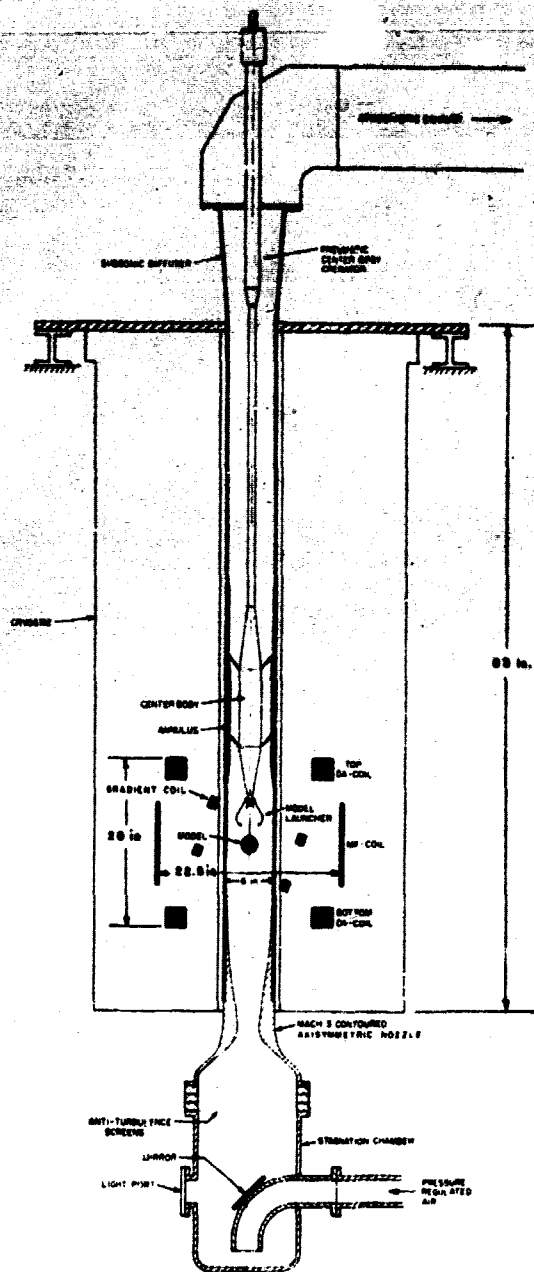


Fig. 2 Sketch of the Prototype Facility

### The Magnetic Suspension

The coil assembly is a realization of Parker's  $\tan^{-1} \sqrt{8}$  orthogonal configuration (5). The basic suspension element is a spherical core imbedded in the aerodynamic model and magnetized uniformly when placed in a uniform magnetic field. Forces are exerted on the sphere by pure magnetic field gradients produced by pairs of coils, with a common symmetry axis, placed symmetrically about the sphere, and with equal but opposite currents. Direction and magnitude of these forces depend on the angle between the gradient coil axis and the direction of magnetization of the sphere. The

present configuration produces forces aligned with the sides of a cube whose diagonal coincides with the vertical axis. In addition to the basic  $\tan^{-1} \sqrt{3}$  gradient coils there is a pair of gradient coils whose symmetry axis coincides with the tunnel axis, to balance the average drag force on the suspended model. The magnetizing Main Field (MF) coil and the two Drag Augmentation (DA) coils operate in a d.c. mode. The six Gradient (GRAD) coils, needed for stability in all directions, operate in an unsteady, or a.c., mode. Figure 3 is a scale drawing of the coil assembly mounted inside the cryostat. One of the three gradient coil pairs is shown. All coils are mounted rigidly with respect to each other by means of bolted fiberglass-epoxy forms capable of withstanding the rather large intercoil forces produced when the suspension is operating. The most important design details of the three types of coils used in this suspension are summarized in Table 1.

In Figure 3 a dimensional sketch of the cryostat and associated hardware is included. Note the rather complex construction of the liquid helium and liquid nitrogen dewars necessary to have a room temperature wind tunnel access through the center of the cryostat. Note also the poor accessibility to the wind tunnel test section resulting from an attempt to place the coil assembly as close to the model as possible. (However, this difficulty should be greatly alleviated in larger facilities.) Also shown in the figure are the fixed temperature sensors, used primarily as indicators of liquid helium level at fixed locations, and one of the vapor-cooled leads, specially designed to minimize helium boil-off due to Joulian losses in these current-carrying leads. In fact, all helium vapor produced during an experiment is conveyed out of the cryostat through these leads, thus making optimum use of the cooling capability of helium vapor.

A basic aspect of the magnetic suspension concept is the feedback control of currents in the support coils to keep the suspended model in the desired position, or, to make the model undergo prescribed motions. To implement this, the instantaneous position of the model must be observed and the resulting information processed by the control system. The most widely used position sensing devices are optical in nature and work in conjunction with photoelectric transducers to generate appropriate control signals. These optical devices are inherently model-shape dependent which means that ad-hoc modifications are required for every model change. On the positive side, optical

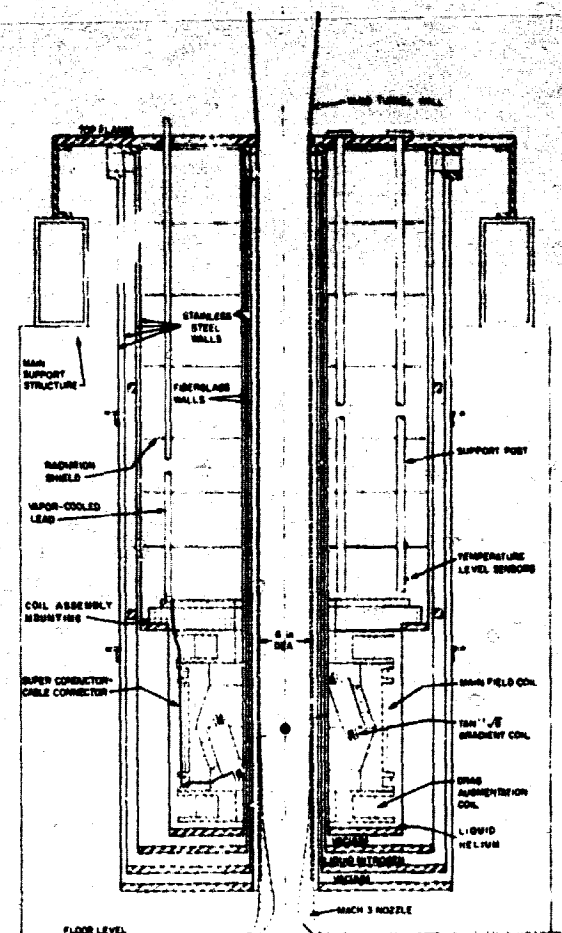


Fig. 3 Magnetic Suspension Details

detectors are relatively straightforward to design and operate and have been made significantly more attractive with the advent of steady state laser light sources. After an unsuccessful attempt to incorporate an electromagnetic position sensing device which in principle is model-shape independent, a laser-source optical system was adopted for this prototype facility. Three 2-beam optical axes are operated from a single 7 mwatt helium-neon

Table 1 Prototype Coil Characteristics

COIL TYPES	GRAD	DA	MF
PROPERTIES			
Number of coils in assembly	6	2	1
Number of turns/coil	135	3200	2500
Dimensions, OD/JD/L (cm)	20/13/1.3	51/38/6.4	57/55/25
Type of superconductor	GE-150 NbSn tape	0.076 cm copper clad NbTi	
Type of operation	a.c.	d.c.	d.c.
Measured resistance room temp/1 He temp ( $\Omega$ )	1.9/0.0012 (1 coil)	423/0.0033 (2 coils)	203/0.0036
Measured inductance room temp/1 He temp ( $\Omega$ )	$3.9 \times 10^{-3} / 3.6 \times 10^{-3}$ (1 coil)	7.6/4.4 (2 coils)	2.2/1.6
Measured Q-factor room temp/1 He temp ( $\Omega$ )	8/25	2.1/4.2	2.2/2.6
Maximum design current (A)	350	100	100
Maximum mag. field at NSP (G) (1 coil)	575	3200	6100
Maximum mag. field gradient at NSP (G/cm) (1 coil)	36	210	0

laser by means of conventional mirror and beam splitter arrangements. Figure 4 shows the optical path of one of the six light beams as an illustration of the system arrangement and the practical difficulties of observing the model. Visual access to the model is available through a remote viewer - coherent fiber optics cable arrangement whose output image can be viewed directly on a screen or on a closed circuit TV monitor.

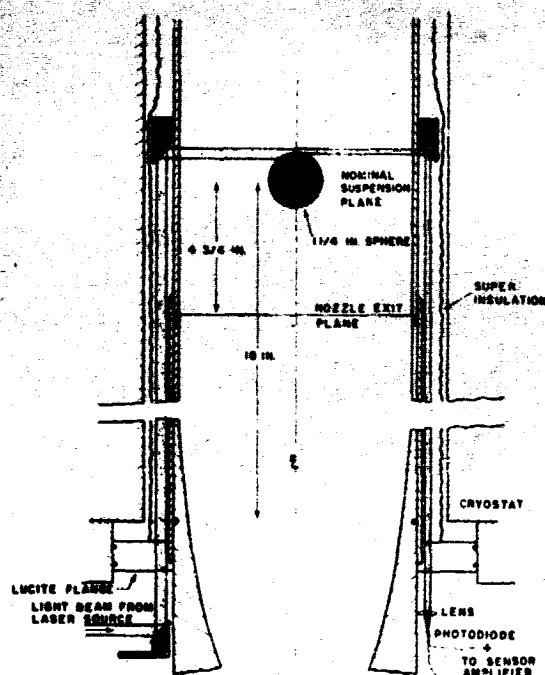


Fig. 4 Sketch of Optical Sensor Channel

A block diagram of the complete feedback control loop is shown in Figure 5. The main difference between this and other magnetic suspension control circuits is the need for a linear coordinate transformation circuit which transforms signals related to model motion in the wind tunnel coordinate system into control signals appropriate to the  $\tan^{-1} \sqrt{8}$  coil coordinate system. Note also that for models not magnetized to saturation, the magnetization level induced in the model by the main field coil contributes directly to the overall loop gain, and hence it is an additional factor influencing the dynamic characteristics of the system. Figure 6 shows a sample of dynamic response curves obtained by perturbing the closed loop system with sinusoidal signals for different levels of magnetization of the suspended model.\*

#### Operational Characteristics

Before discussing the system capabilities as a wind tunnel magnetic suspension and balance, it

At the time these dynamic response measurements were made the system was plagued with low frequency vibration noise which was subsequently eliminated. Hence, the curves in Figure 6 are given for illustrative purposes only and are not representative of the full dynamic capability of the system.

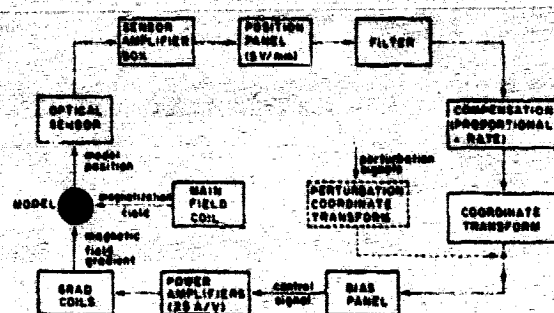


Fig. 5 Block Diagram of Control System

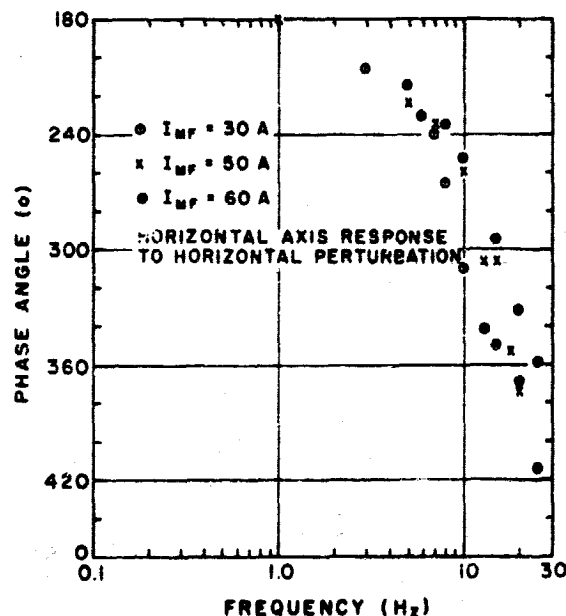
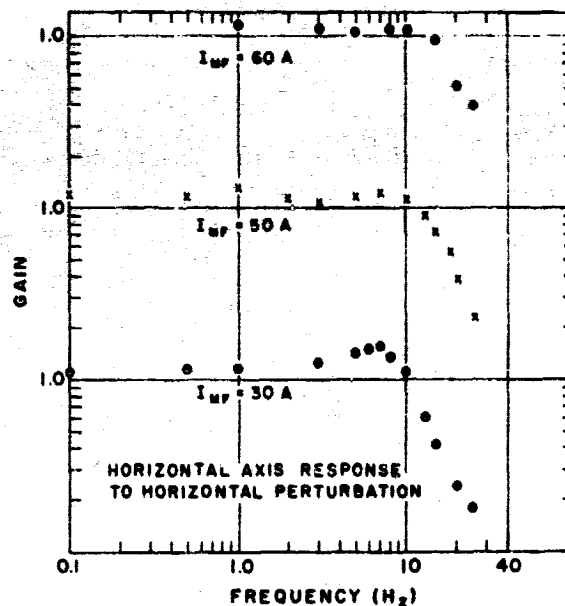


Fig. 6 Sample of System Dynamic Response (1 in. iron sphere suspended)

is appropriate to describe some of its unique operational characteristics related to the use of superconductor technology. Principally, time becomes a very important parameter when this facility is operated, both before and during the actual aerodynamic experiment. A precooling period of about 36 hours is necessary to prepare the facility for economic liquid helium transfer (about 800 liters of liquid nitrogen are used for precooling). Normally it takes about 4 hours between liquid helium transfer starts and the first experiment can be run. From this point, about 8 hours of run time are available before additional helium has to be transferred. A two-day experiment will consume between 400 and 500 liters of liquid helium and yield between 12 and 16 hours of useful run time. With the available air storage-wind tunnel combination a maximum of 10 4-minute runs at Mach 3 can be accommodated in this period. It should be apparent that better-than-usual experiment planning is required for economic utilization of the facility.

Another important operational characteristic is the potential danger of operating relatively high energy coils in liquid helium environment. In fact, safety must be a primary concern vis-a-vis the design and operation of a facility such as this. For example the power supplies for the larger coils (main field and drag augmentation) are equipped with protective circuit components to prevent sudden changes in the magnitude of the supplied currents. The pressure inside the liquid helium dewar is constantly monitored and adequate pressure relief devices are available for emergency situations.

One of the principal advantages claimed for the coil configuration adopted for this facility is the linearity of the relationships between the magnitudes of support coil currents and magnetic forces exerted on supported models. This characteristic makes the magnetic suspension an attractive wind tunnel balance (a 3-component balance in this particular case). In the most general case, all three types of coils in the prototype configuration can exert forces on a magnetized model. In the sketch of Figure 7, the ferromagnetic sphere is shown suspended a distance  $\Delta x$  above the nominal suspension point. Hence, for small  $\Delta x$  (6):

$$\begin{aligned}
 F_{MAG,x} &= F_{DA} + F_{MF} + F_{GRAD} \\
 &= \mu_0 MV \left( \left( \frac{\partial B}{\partial x} \right)_{NSP,DA} + \Delta x \left( \frac{\partial^2 B}{\partial x^2} \right)_{NSP,MF} \right. \\
 &\quad \left. + k \left( \frac{\partial B}{\partial x} \right)_{NSP,GRAD} \right) \\
 &= \alpha W I_{MF} I_{DA} + \beta \Delta x W I_{MF}^2 + \gamma W I_{MF}^2 I_{GRAD}
 \end{aligned}$$

where  $F$  represents force,  $M$  is the intrinsic magnetic moment per unit volume induced in the sphere by the main field,  $V$  is the sphere volume,  $B$  represents magnetic induction,  $x$  and  $z$  are axial coordinates (see Figure 7),  $W$  is the sphere weight,  $I$  represents electric current and  $\alpha$ ,  $\beta$ , and  $\gamma$  are constants for a fixed geometric coil configuration, and where it has been assumed that the model magnetization increases linearly with main field

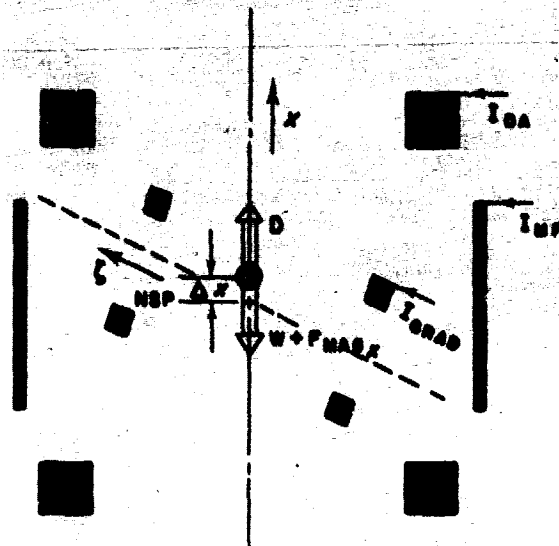


Fig. 7 Sketch of Magnetic Balance Forces

current  $I_{MF}$ . Note that, to a first order approximation, there is a vertical force exerted on the model by the magnetization coil which is proportional to the magnitude of the vertical misalignment of the model with respect to the nominal suspension point. Note also that, in general, all three gradient coil pairs contribute to the vertical force linearly. Finally, it is worth noting that the above force equation is basically a vector equation, i.e., the directions of the contributions of the drag augmentation coils and the gradient coils depend on the directions of current flow through such coils (or coil magnetic polarities) with respect to the current flow (or polarity) of the main field coil. Vertical displacement of the model always produces a force in a direction opposite to the displacement.

The magnitudes of the constants  $\alpha$ ,  $\beta \Delta x$ , and  $\gamma$  were determined by a detailed calibration of the magnetic balance in which a 1.25 inch model was suspended by a string from a load cell (simulating the drag force on the model) and stabilized laterally near the nominal suspension point by the magnetic suspension. Main field current was used as a parameter while drag augmentation current was varied over a wide range of values for the two polarities of the gradient coils relative to that of the main field coil. Results are summarized graphically in Figure 8. Linearity is excellent throughout. Constants  $\alpha$  and  $\gamma$  have experimental uncertainties of less than 1 and 5% respectively. The much larger uncertainty associated with the determination of  $\beta \Delta x$  is undoubtedly due to insufficient care in holding  $\Delta x$  constant from one experiment to the next. However, this should present no serious practical problems in actual operation for two reasons: First, the magnitude of the contribution of the main field coil to the overall vertical force is small compared to the contributions by drag augmentation and gradient coils for values of  $D/W$  in the range of operating conditions for supersonic flow. Second, by careful adjustment of optical sensor components,  $\Delta x$  can be made arbitrarily small and thus,  $F_{MF}$  can be made vanishingly small even for moderate and low

D/W situations. In the present case, before any adjustments were made, a measurement of sphere drag at a very low value of D/W yielded results in good agreement with those obtained via other experimental techniques (see Table 3).

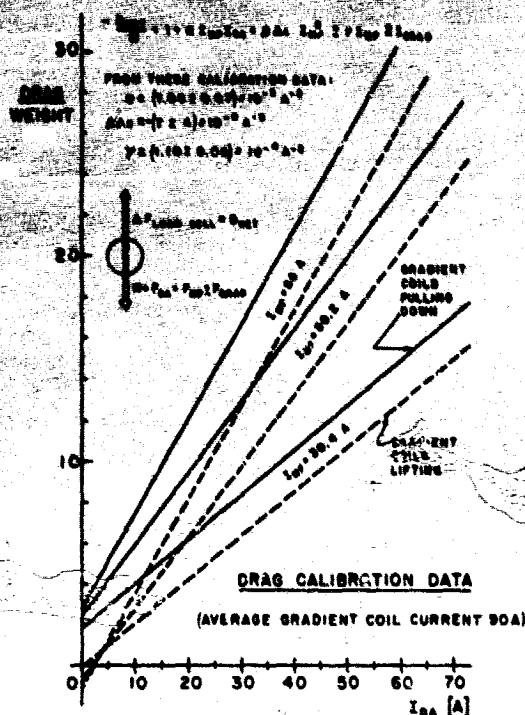


Fig. 8 Drag Calibration Results

Table 3 Summary of Subsonic Sphere Drag Measurement

Stagnation pressure	1 atm
Dynamic pressure	0.00145 atm (1.5 cm H <sub>2</sub> O)
Sphere diameter, d	1.25 in
Reynolds number based on d	$3.2 \times 10^4$
Mach number	0.045
Measured D/W	0.043
Computed value of $C_D$	0.48
Commonly accepted value (7)	0.47

Based on the above calibration results, the range of drag augmentation and main field current settings necessary for supporting a 1.25 in. sphere in Mach 3, 48 psia stagnation pressure air flow have been computed and are listed in Table 4. Note that the average magnitude of the current in each gradient coil pair has been assumed at mid-range, i.e., 175 A for a total of 525 A for all three pairs.

At the start of this project there were strong doubts among applied superconductivity experts concerning the feasibility of operating superconductor coils in the tightly coupled dynamic environment typical of magnetic suspension systems. The key question concerned the level of energy dissipation by the coils resulting perhaps in unacceptable helium boil-off rates or even loss of superconductivity properties in

extreme cases. The principal contribution claimed in this paper consists of proving conclusively that superconductors can be used for wind tunnel magnetic suspensions, under rather severe dynamic conditions, and that helium boil-off levels are quite acceptable even without the significant facility design improvements that appear possible. As with all new facility concepts, the need to use new technology or to use old technology in new ways often resulted in unpredictable noisy and/or unstable behavior of the system, imposing on the coils dynamic conditions far more demanding than those anticipated for normal wind tunnel operation. This, in retrospect, is fortunate because it adds a substantial safety margin to this demonstration of feasibility.

Table 4

Current Settings for Mach 3, 48 psia Flow  
(D-W/W = 33.86, assuming  $C_D = 1$ ,  $d_{\text{SPHERE}} = 1.25$ )

$I_{MF}$ (A)	$\gamma$	$I_{MF} \Sigma I_{GRAD}$	needed $I_{MF} I_{DA}$	needed $I_{DA}$ (A)
60	3.21	30.66		78.2
65	3.48	30.39		71.6
70	3.75	30.12		65.9
75	4.02	29.85		60.9
80	4.28	29.59		56.6

A quantitative measure of energy dissipation in the prototype facility is obtained by monitoring the combined volumetric flow rate out of all vapor-cooled current leads by means of a calibrated turbine flow meter. Typical results of such measurements are displayed in Figure 9, including the boil-off rate corresponding to operation of one gradient coil pair under extreme dynamic conditions. It should be noted that the nature of the gradient coil power amplifiers coupled with the overall complexity of the control circuit in the prototype facility results in a relatively large high frequency content in the gradient coil currents. Thus results shown in Figure 9 represent a worst case which can be improved by appropriate filtering and other control circuit refinements.

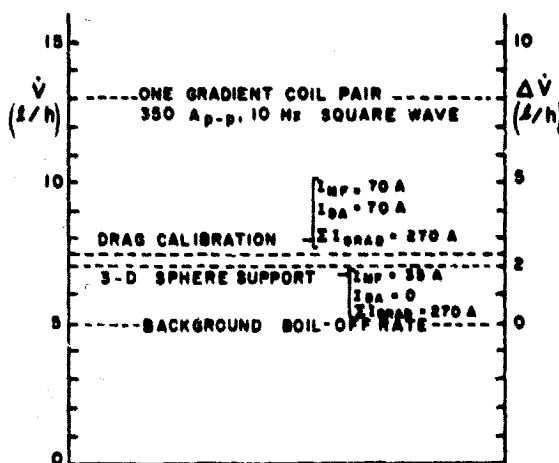


Fig. 9 Typical Helium Dissipation Rates



### Scaling to Large Systems

Before extrapolating design and operational characteristics of the prototype facility to larger scale facilities, a redesign of the prototype coil assembly was carried out to take advantage of opportunities created by changes made during the development of the facility and lessons learned during the shake down and testing process. The principal changes that would be implemented in a new coil system are: (1) the main field coil would be split into a Helmholtz-like pair of coils with the same polarity to improve the uniformity of the magnetizing field in the vicinity of the nominal suspension point, and (2) the drag augmentation coils would be moved closer to the suspension point and their windings would be located at a more favorable angle with respect to the coil axis, thus increasing the axial field gradient at NSP by nearly 50%. On the whole these changes result in a substantially more compact coil assembly than that of the existing prototype facility. This improved prototype design has been taken as the basis for the extrapolations discussed below.

The main purpose of this design extrapolation exercise is to estimate realistically the order of magnitude of coil size and liquid helium consumption requirements for large scale aerodynamic test facilities. Furthermore, it is useful to explore the advantages of combining a superconductor magnetic suspension and balance with a cryogenic wind tunnel. It must be pointed out, however, that no specific aerodynamic tests are being considered herein and, hence, it would be premature to decide on any particular coil configuration as being optimal in some sense. Rather, all calculations are made for a  $\tan^{-1} \sqrt{8}$  configuration with drag augmentation similar to that of the improved prototype design. Also, a simple spherical model is used in the calculations as an adequate representative of the scale of more realistic aerodynamic shapes. Again, results presented below should be considered realistic from the point of view of order of magnitude only.

To understand the coil scaling process it should be kept in mind that for a given geometric coil configuration, the magnitude of the magnetic force exerted by a pair of gradient coils on a magnetized sphere is of the form:

$$F_{\text{MAG}} = kVM \frac{\partial B}{\partial x}$$

where  $V$ ,  $M$ , and  $\frac{\partial B}{\partial x}$ , have been defined before in this paper and  $k$  is a constant whose magnitude depends on the geometry of the gradient coil windings relative to the direction of magnetization and position of the sphere. Of course, in the case of air-core coils the magnitudes of magnetic fields and their gradients are simply proportional to the magnitudes of the respective currents. At the same time, aerodynamic forces are approximately proportional to the cross sectional area of a model. For example, for a sphere of diameter  $d$  the drag force exerted by a flow characterized by a dynamic pressure  $q$  is:

$$D = C_D q \frac{\pi d^2}{4}$$

From the scaling laws summarized in Figure 1 it follows that the magnitudes of magnetic field gradients remain constant for similar coil

geometries while the magnitudes of magnetizing fields scale linearly with the coil characteristic dimension. Thus, assuming that the supported sphere's magnetization increases linearly with magnetizing field (a good approximation for iron in the range of magnetic field intensities of interest here), a practical expression for computing coil size requirements for larger but similarly shaped coil configurations is:

$$\frac{q_1}{q_2} = \left(\frac{d_2}{d_1}\right) \times \lambda \left(\frac{NI_2}{NI_1}\right)_{\text{MF}} \times \frac{(NI_2)_{\text{DA}} + c(NI_2)_{\text{GRAD}}}{(NI_1)_{\text{DA}} + c(NI_1)_{\text{GRAD}}} = 1$$

where  $\lambda$  is the coil scaling factor (different, in general, from the model scaling factor) and  $c$  represents the relative steady state contribution by the gradient coils to the magnetic force checking aerodynamic drag. The contribution by the model weight has been neglected in this expression. Current density levels are assumed to remain unchanged and, hence, coil volumes scale with the magnitude of the product  $\lambda \left(\frac{NI_2}{NI_1}\right)$ .

Coil size is important for three reasons. First, coil and cryostat costs should be dependent on size at least linearly. Second, steady state helium evaporation losses are expected to depend on wetted area and, hence, to scale roughly with the square of the coils (and therefore cryostat) characteristic dimension. Third, a.c. losses of gradient coils appear to scale linearly with the frequency of the changing current and the length of wound superconductor. To corroborate the latter assumption a series of a.c. losses experiments for a set of coils wound with the same superconductor tape used in the prototype gradient coils are being conducted in our laboratory. Typical results for two coils tested separately and jointly are shown in Figure 10. A wide range of frequencies and currents are represented in these results which seem to confirm a.c. losses of the form:

$$\frac{E}{f \times l} \sim I^\delta$$

where  $E$  is the rate of energy dissipation measured in terms of helium evaporation rate,  $f$  is the frequency of the sinusoidal coil excitation,  $l$  is the total length of superconductor in the windings,  $I$  is the r.m.s. magnitude of the excitation, and  $\delta$  has a value typically between 2.0 and 2.5 (8).

In the design extrapolations discussed below it has been assumed that current magnitudes and frequencies will be the same for larger facilities as they are for the prototype facility, such that coil size and windings cross section are the only variables available to the designer. This is perhaps an unnecessarily conservative assumption since, for example, there is good reason to expect substantially lower characteristic operating frequencies in larger facilities. Also, somewhat more complicated trade-off calculations would in all probability yield more favorable combinations of sizes and current levels for gradient coils. However, given the intent of the present preliminary design calculations it makes sense to take this worst case approach as a safety factor.



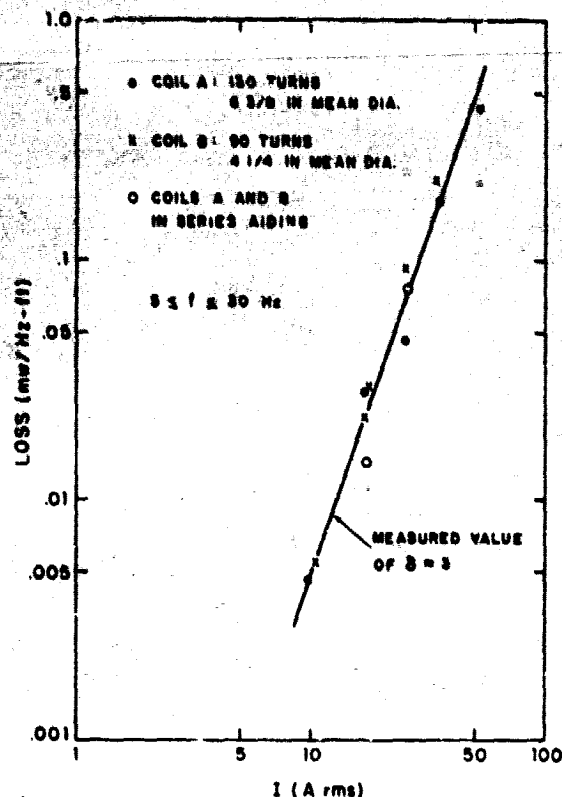


Fig. 10 Sample Data From a.c. Losses Scaling Tests

#### Scaling to Langley Cryogenic Transonic Pilot Tunnel

This is a highly successful fully operational facility developed at NASA Langley Research Center to explore the design, operational, and research characteristics of the high Reynolds number cryogenic wind tunnel concept (9). From the point of view of exploring extensions of the superconductor magnetic suspension technique to large scale facilities it offers the two main advantages of cryogenic wind tunnels, i.e., drastically reduced aerodynamic loads for a given Reynolds number (low  $q$ ), and a cryogenic environment in the test section which simplifies the cryostat design and promotes relative reduction of coil size. This particular facility offers the additional advantage of being of intermediate size, thus giving the designer added confidence in the validity of his design extrapolation.

A larger size, octagonal test section has been assumed available as a modification of the Transonic Pilot Tunnel, for the purposes of this exercise. An extreme (but realistic) flow condition has also been assumed. Results are presented in Table 5. A scale sketch of the respective coil configurations is given as Figure 11 where the relative coil size reduction is evident, particularly for GRAD and DA coils. Thus, for example, although model volume increases by a factor of 64 and drag capability by a factor of 50, gradient coil volume and helium boil-off increase only by a factor of 8.

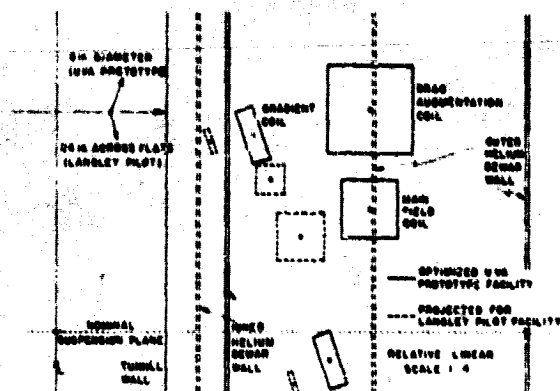


Fig. 11 Dimensional Sketch of Design Extrapolation

#### Scaling to Langley Cryogenic Transonic Research Tunnel

This is a truly large scale facility still in the design state at Langley Research Center. The only purpose of speculating this far into an as yet uncertain future is to explore to a practical upper limit the relative advantages of scaling a superconductor magnetic suspension while at the same time getting crude upper limit estimates of helium consumption. The last column in Table 5 summarizes the results of calculations based on straight extrapolation from the design for the Langley pilot facility. That is, no further relative reduction in cryostat or coil size is assumed. Estimated coil sizes and helium losses are expectedly quite large but do not appear forbidding in view of the size of the overall test facility. Furthermore, considerable improvements should be possible by a more elaborate design optimization process.

#### Conclusions

Successful development and operation of a superconductor magnetic suspension and balance prototype facility at the University of Virginia has proven the feasibility of applying this useful experimental technique to large scale aerodynamic testing. This type of application should be particularly attractive when the advantages of magnetic suspensions and cryogenic wind tunnels are combined, as shown by the results of preliminary design estimates for a magnetic suspension configuration compatible with NASA Langley Transonic Pilot Tunnel and extrapolated projections for the planned Transonic Research Tunnel. Although calculations were made only for magnetic coil configurations similar to that of the University of Virginia prototype, results should be order-of-magnitude valid for other magnetic suspension configurations as well.

Design and operational data and experience accumulated during the development and testing of the prototype facility point to several problem areas where effort should be rewarded with substantial improvement of the effectiveness of this experimental technique. These problem areas are:

Table 5 Summary of Design Extrapolations to Large Scale Aerodynamic Facilities

PARAMETERS RELEVANT TO FACILITY SCALING	OPTIMIZED UVA PROTOTYPE	FOR LANGLEY TRANSONIC PILOT TUNNEL	FOR LANGLEY TRANSONIC RESEARCH TUNNEL
1. TUNNEL GEOMETRY shape of test section size (in)	circular diameter: 5 3/4	octagonal across flats: 24	octagonal across flats: 96
2. MODEL SCALING diameter: d projected area: $\sim d^2$ volume: $\sim d^3$	1 1 1	4 16 64	16 256 4096
3. FLOW CHARACTERIZATION Mach number stagnation pressure (psia) dynamic pressure (psi)	3 50 8.6	1 73.5 27.2	1 60 22.2
4. SPHERE DRAG SCALING	1	50	660
5. COIL GEOMETRIES (MF/DA/GRAD) mean diameter (in) cross section (sq in) volume (cu in) mean half angle to axis (deg)	17.3/17.3/6.50 2.48/5.59/0.75 135/304/15.3 69/55/25	53.75/47.2/28 25/10/1.38 4230/1485/122 69/55/31	214/189/112 100/32/44 67750/19000/1560 69/55/31
6. HELIUM ANNULUS GEOMETRY inner wetted diameter (in) outer wetted diameter (in)	9.5 26	31.5 70	126 280
7. MAGNETIC FIELD SCALING required drag capability model volume factor model magnetization factor drag augmentation factor gradient coil factor	1 1 1 1 1	50 64 3.25 .24 .24	660 4096 3.25 .05 .05
8. HELIUM BOIL-OFF scaling factor for background losses scaling factor for gradient coil losses boil-off rate: (background/gradient coils/total) (l/hr)	1 1 1 5/5/10	8.2 7.9 41/39/80	131 102 655/510/1165

(1) Power supplies for active support coils. Two immediate benefits will accrue from "smoother" power amplifiers, i.e., lower liquid helium evaporation rates and removal of the main obstacle in the way of a truly effective electromagnetic model position sensor.

(2) Shape-independent model position sensor. This important aspect of magnetic suspension systems is related to the power supply problem, and should be approached accordingly.

(3) Cryostat design. As facilities become larger, background helium evaporation rates become significant. It is felt that much improvement can be made in this area. Also, the questions of tunnel accessibility and convertibility from a magnetic suspension mode to other tunnel operating modes must be examined in detail for large scale facilities.

Concerning the combination of superconductor magnetic suspensions and cryogenic wind tunnels, much detailed work needs to be done to arrive at an optimal interface design which will yield the anticipated advantages of this potentially very attractive facility concept.

(4) Safety and reliability. Again, the safety problem becomes more important as the scale

of the facility grows larger. The area of reliability of magnetic suspension of wind tunnel models (as models become larger and more expensive) has not been studied in detail so far, but the economic incentive of doing so for larger systems is obvious.

(5) a.c. losses in superconductors. This does not appear to be as serious a problem as it was feared at the start of this project. However, helium consumption can reach substantial levels in large facilities and a careful search for the most suitable superconductor available should be conducted for every new system.

In view of the above, one cannot escape the conclusion that the logical next step should be to build a medium size facility where the design extrapolation estimates and the suggested improvements can be tested. All the necessary technology to carry out this next step is available today. Ideally, this intermediate scale facility would combine a superconductor magnetic suspension with a cryogenic wind tunnel, thus enabling sufficiently high Reynolds number experiments to be performed to assess quantitatively the merits of free-support aerodynamic testing in realistic flight simulation environments. The implementation of such proposal should prove a challenging and rewarding endeavor.

### References

1. Clemens, P. L. and Cortner, A. H., Bibliography: The Magnetic Suspension of Wind Tunnel Models, AEDC Report TDR-63-20, February 1963.
2. Summary of ARL Symposium on Magnetic Wind Tunnel Model Suspension and Balance Systems, ARL Report 66-0135, edited by F. L. Daum, July 1966.
3. Proceedings of the Second International Symposium on Electromagnetic Suspension, University of Southampton report edited by M. Goodyer and M. Judd, 1972.
4. Covert, E. E., et al., "Magnetic Balance and Suspension Systems for Use with Wind Tunnels," chapter 2 of Progress in Aerospace Sciences, Volume 14, pp. 27-107, edited by D. Kuchemann, Pergamon Press, 1973. (This reference represents a brief but quite complete review of the basic principles, design concepts, and applications of magnetic suspension techniques for aerodynamic testing, and includes rather extensive reference lists.)
5. Parker, H. M., pp. 137-157 in reference 2.
6. Dukes, T. A., and Zapata, R. N., "Magnetic Suspension with Minimum Coupling Effects for Wind Tunnel Models," Transactions IEEE, (AES-1) vol. 1, pp. 20-28, August 1965.
7. Fluid-Dynamic Drag, Sigvard F. Howner, 1965 (published by author).
8. Moss, F. M., paper C in reference 3.
9. Kilgore, R. A., et al., "Flight Simulation Characteristics of the Langley High Reynolds Number Cryogenic Transonic Tunnel," AIAA Paper No. 74-80, 125th Aerospace Sciences Meeting, Washington, D. C., January 1974.

### Acknowledgments

A fond and respectful tribute is due to the late Harleth Wiley who as Head of the Vehicle Dynamics Section of the High Speed Aircraft Division of NASA Langley Research Center promoted, encouraged, and supported in every way available to him the development of our prototype facility. His faith in the validity and viability of the magnetic suspension concept as applied to large scale aerodynamic testing was a powerful force which carried us through difficult periods in this project. His dream of a large scale facility fulfilling its appropriate role in aerodynamic testing will come true in the future; and although he will not be physically present to enjoy its realization, his memory will be very much in the minds of those of us at the University of Virginia, at Langley and elsewhere who were privileged to share such a dream with him.